




Cite this: *RSC Adv.*, 2017, 7, 29697

# A turn-on fluorescent chemosensor based on acylhydrazone for sensing of $Mg^{2+}$ with a low detection limit†

Jing-Han Hu, \* Jian-Bin Li, You Sun, Peng-Xiang Pei and Jing Qi

A novel highly selective chemosensor for  $Mg^{2+}$  ions based on the naphthalene group as the fluorophore has been designed and synthesized, which shows a fluorescence turn-on response from colorless to green for  $Mg^{2+}$  ions in DMSO– $H_2O$  solutions. L could perform as an “OFF–ON” molecular switch, which was cyclically controlled by  $Mg^{2+}$  and EDTA. Moreover, further study demonstrated that the detection limit for the fluorescence response of L to  $Mg^{2+}$  was down to  $9.2 \times 10^{-10}$  M, which was lower than with other sensors for  $Mg^{2+}$ . Test strips based on L were also fabricated, which could act as a convenient and efficient  $Mg^{2+}$  test kit. The sensor L could detect  $Mg^{2+}$  in two different sources of water, distilled and tap water.

Received 20th April 2017  
 Accepted 24th May 2017

DOI: 10.1039/c7ra04462c  
[rsc.li/rsc-advances](http://rsc.li/rsc-advances)

## Introduction

The magnesium ion ( $Mg^{2+}$ ) plays vital roles in biological systems.<sup>1–3</sup> For plants, magnesium is one of the ingredients for forming chlorophyll and is involved with forming phosphate compounds and phosphate metabolism.<sup>4,5</sup> In the cells of the human body,  $Mg^{2+}$  is one of the most abundant cations, and participates in numerous basic biochemical reactions. Magnesium also plays a crucial role in skeletal development and bone remodeling.<sup>6,7</sup> Magnesium ion can influence nervous impulses and tension development in muscle, and modulates, amongst others, ion transport in nerves and mitochondria.<sup>8–10</sup> If the concentrations of magnesium in the cytosol and subcellular regions are abnormal, there is a possibility of the occurrence of a disease, such as diabetes, hypertension, epilepsy and Alzheimer’s disease.<sup>11–13</sup> In particular, detection of  $Mg^{2+}$  has been of considerable interest and a great amount of effort has been devoted to the design and synthesis of sensitive and selective sensors for  $Mg^{2+}$  ion.

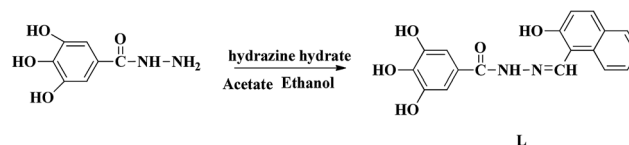
Nonetheless, reports about fluorescent sensors for  $Mg^{2+}$  are still few compared with those on other important ions, such as  $Zn^{2+}$ ,  $Al^{3+}$ ,  $Hg^{2+}$  and  $CN^-$ .<sup>14–27</sup> Even so, some methodologies for detecting  $Mg^{2+}$  are often interfered with by  $Zn^{2+}$  and  $Ca^{2+}$ . To date, as far as we know,  $\beta$ -diketone, crown ether derivatives, and nanoparticles have been employed for selective detection of  $Mg^{2+}$  ions.<sup>28–30</sup> It is worth mentioning that their synthetic processes are intricate. Hence, there is interest in designing a highly selective, sensitive and simple chemosensor that

recognizes  $Mg^{2+}$  without the interference of other metal ions.<sup>31,32</sup>

Our research group has a longstanding interest in molecular recognition.<sup>33–38</sup> We have successfully developed a simple and efficient optical fluorescent acylhydrazone chemosensor L that can detect  $Mg^{2+}$  in DMSO– $H_2O$  solution. To the best of our knowledge, acylhydrazone is easy and inexpensive to prepare. The naphthalene group acts as the fluorophore, while the hydroxyl and imine groups in the sensor molecule L enhance the coordination capacity. As a result, the addition of  $Mg^{2+}$  inhibits the ESIPT process and increases its structural rigidity, which leads to a strong green emission. The mechanism of this process was verified by spectroscopic methods, including <sup>1</sup>H NMR, DFT and mass spectrometry. The fluorescent detection limit of the sensor for  $Mg^{2+}$  was  $9.2 \times 10^{-10}$  M, while the corresponding detection limit by the naked eye was determined to be  $5.0 \times 10^{-8}$  M under a UV lamp at 365 nm.

## Results and discussion

The molecule L was conveniently synthesized *via* the condensation of 3,4,5-trihydroxybenzhydrazide and 2-hydroxy-1-naphthaldehyde. The recognition abilities of L were investigated by adding perchlorate salts ( $Fe^{3+}$ ,  $Hg^{2+}$ ,  $Ag^+$ ,  $Ca^{2+}$ ,  $Cu^{2+}$ ,  $Co^{2+}$ ,  $Ni^{2+}$ ,  $Cd^{2+}$ ,  $Pb^{2+}$ ,  $Zn^{2+}$ ,  $Cr^{3+}$  and  $Mg^{2+}$ ) into DMSO– $H_2O$  solutions (Scheme 1).



Scheme 1 Synthesis of receptor L.

College of Chemical and Biological Engineering, Lanzhou Jiaotong University, Lanzhou, Gansu, 730070, P. R. China. E-mail: [hujinghan62@163.com](mailto:hujinghan62@163.com)

† Electronic supplementary information (ESI) available: Complete experimental procedures and some of the spectroscopic. See DOI: 10.1039/c7ra04462c



Receptor **L** was found to have limited solubility in water, and this compelled us to use this sensor in mixed solvents. The fluorescence emission was examined upon adding various metal ions:  $\text{Fe}^{3+}$ ,  $\text{Hg}^{2+}$ ,  $\text{Ag}^+$ ,  $\text{Ca}^{2+}$ ,  $\text{Cu}^{2+}$ ,  $\text{Co}^{2+}$ ,  $\text{Ni}^{2+}$ ,  $\text{Cd}^{2+}$ ,  $\text{Pb}^{2+}$ ,  $\text{Zn}^{2+}$ ,  $\text{Cr}^{3+}$  and  $\text{Mg}^{2+}$  ions in DMSO/ $\text{H}_2\text{O}$  (7 : 3, v/v, 0.01 M HEPES, pH = 8.5). Only compound **L** displayed a weak, single fluorescence emission band at 480 nm when excited at 378 nm in DMSO- $\text{H}_2\text{O}$  media. Changes in the spectral pattern were observed only with the addition of 20 equivalents of  $\text{Mg}^{2+}$ , when sensor **L** produced a strong fluorescence band at 480 nm and responded with a dramatic color change, from colorless to green. However, upon addition of other metal ions no significant changes in color were observed (Fig. 1). In addition, the fluorescence emission was also examined upon adding  $\text{MnCl}_2$  and  $\text{CaCl}_2$  (Fig S3†). The addition of  $\text{Mn}^{2+}$  caused no significant spectral change. The absorption spectra of **L** in the presence of other ions were also tested. The results suggested that sensor **L** could display an excellent selectivity for  $\text{Mg}^{2+}$  over all other ions tested (Fig S4†).

It was well known that fluorescent probes for  $\text{Mg}^{2+}$  might encounter interference from other cations, particularly  $\text{Zn}^{2+}$  and  $\text{Cd}^{2+}$ . Thus, competitive behavior was tested to further elucidate whether the coexistence of competing metal cations interfered with the detection of  $\text{Mg}^{2+}$ . In the solutions of sensor **L** with  $\text{Mg}^{2+}$ , when solutions of **L** were added to solutions of other competing cations, it was clear that the receptor **L** was highly selective for the detection of  $\text{Mg}^{2+}$  in DMSO/ $\text{H}_2\text{O}$  (7 : 3, v/v, 0.01 M HEPES, pH = 8.5) (Fig. 2).

As shown in Fig. 3, the fluorescence titration of  $\text{Mg}^{2+}$  was performed using a 20  $\mu\text{M}$  solution of **L** in DMSO/ $\text{H}_2\text{O}$  (7 : 3, v/v, 0.01 M HEPES, pH = 8.5). With the addition of  $\text{Mg}^{2+}$  (0.2 M), a gradual increase in the fluorescence intensity of chemosensor **L** at 480 nm was observed as the  $\text{Mg}^{2+}$  volume increased from 0 to 1.7 equivalents. The solution containing  $\text{Mg}^{2+}$  also showed a change in fluorescence color from colorless to grass green.

The detection limit is one of the most important parameters in ion sensing. For various practical purposes, it is very

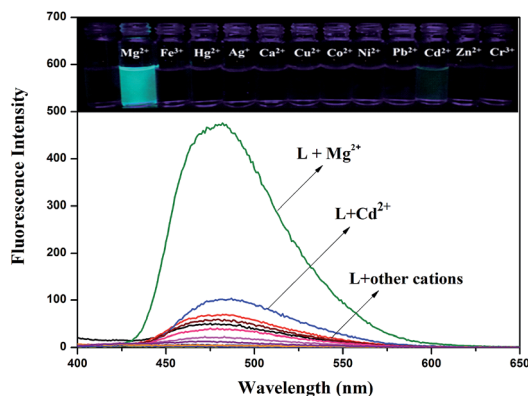


Fig. 1 Fluorescence spectra response of **L** ( $2.0 \times 10^{-5}$  M) in DMSO/ $\text{H}_2\text{O}$  (7 : 3, v/v, 0.01 M HEPES, pH = 8.5) upon addition of  $\text{Mg}^{2+}$ . Inset: photograph in the presence of various cations under UV-lamp (365 nm).

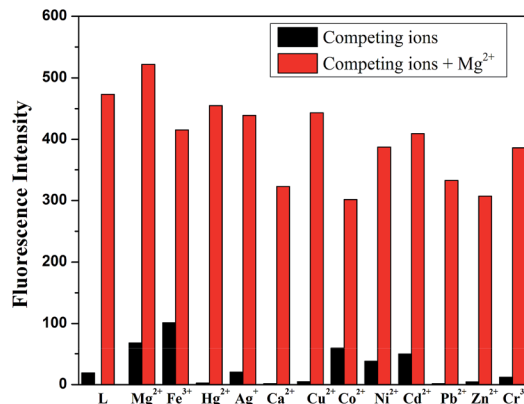


Fig. 2 Fluorescence spectra response of **L** ( $2.0 \times 10^{-5}$  M) in the presence of various cations in DMSO/ $\text{H}_2\text{O}$  (7 : 3, v/v, 0.01 M HEPES, pH = 8.5) in response to  $\text{Mg}^{2+}$ .

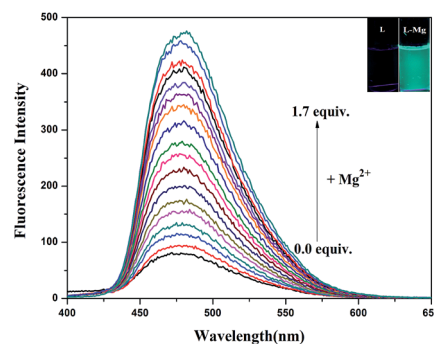


Fig. 3 Fluorescence titration spectra of **L** ( $2.0 \times 10^{-5}$  M) in DMSO/ $\text{H}_2\text{O}$  (7 : 3, v/v, 0.01 M HEPES, pH = 8.5) upon adding of an increasing concentration of  $\text{Mg}^{2+}$  ( $\lambda_{\text{ex}} = 378$  nm). Inset: photograph of **L** upon adding of  $\text{Mg}^{2+}$  under UV-lamp (365 nm).

important to detect analytes at low concentrations. The naked eye detection limit for  $\text{Mg}^{2+}$  was determined to be  $5.0 \times 10^{-8}$  M, through use of a UV lamp at 365 nm (Fig. 4). The detection limit for fluorescent spectrum changes was  $9.2 \times 10^{-10}$  M for  $\text{Mg}^{2+}$ , as calculated on the basis of  $3\delta/S$  (where  $\delta$  is the standard deviation of the blank solution and  $S$  is the slope of the

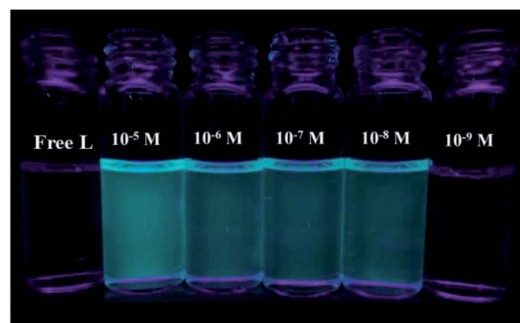


Fig. 4 Naked-eye detection limit under UV light at 365 nm. From left to right the concentration of  $\text{Mg}^{2+}$ :  $10^{-5}$  M,  $5 \times 10^{-6}$  M,  $5 \times 10^{-7}$  M,  $5 \times 10^{-8}$  M,  $5 \times 10^{-9}$  M.



calibration curve), which indicates the high detection sensitivity (Fig. 5). The result of the analysis is as follows: linear calibration equation:  $I = 1.30432C + 53.84714$ ,  $R^2 = 0.997$ .

We also made comparisons with other reported magnesium selective sensors, and the detection limit of **L** was much lower.<sup>29–31</sup> Some did not explain the detection limits. This indicated that probe **L** could be used to quantitatively detect  $Mg^{2+}$  at extremely low concentrations and in a relatively wide range (Table 1).

The pH dependence of the probe **L** system in DMSO/H<sub>2</sub>O (7 : 3, v/v, 0.01 M HEPES, pH = 8.5) was also checked by fluorescence emission spectroscopy.  $Mg^{2+}$  ion was added to buffered solutions of **L** at different pH values (1–12). The probe **L** was insensitive to  $H^+$  and  $OH^-$ . However, the results with the **L**– $Mg^{2+}$  system in DMSO–H<sub>2</sub>O media indicated that the reaction of **L** ( $2.0 \times 10^{-5}$  M) with  $Mg^{2+}$  only occurred effectively in the pH range between 8 and 11, where the fluorescence intensity at

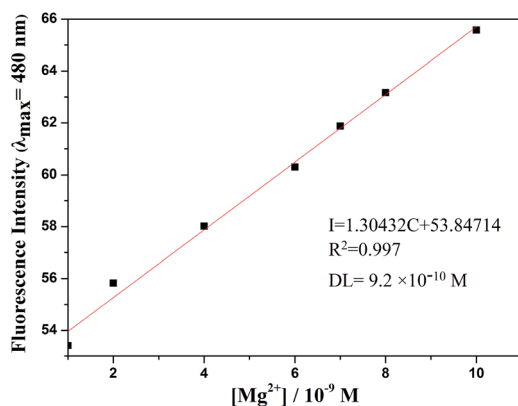


Fig. 5 Fluorescence detection limit spectra of **L** ( $2.0 \times 10^{-5}$  M) in DMSO/H<sub>2</sub>O (7 : 3, v/v, 0.01 M HEPES, pH = 8.5) solution upon adding of a concentration of  $Mg^{2+}$ .

Table 1 Comparison of detection limits

Journal	Structures	Detection limits (fluorometric)	Solvent
This work		$9.2 \times 10^{-10}$ M	DMSO/H <sub>2</sub> O (7 : 3, v/v)
39		$5.16 \times 10^{-7}$ M	Ethanol
40		$1.44 \times 10^{-6}$ M	Acetonitrile
41		$2.37 \times 10^{-8}$ M	Deionized water

480 nm was enhanced more significantly, which indicated that the sensor **L** and  $Mg^{2+}$  ions and formed a magnesium complex in weak alkaline solutions (Fig. S5†).

According to <sup>1</sup>H NMR spectra (Fig. 6), the addition of  $Mg^{2+}$  made the two proton signals of –OH and –NH at 12.96 (s, 1H) and 11.92 (s, 1H) ppm gradually disappear. Due to coordination of the O atom of the carbonyl group in **L**, the signal of the two hydroxyl atoms at 9.29 (s, 2H) ppm in the benzene ring showed a significant downfield shift. To further investigate the interaction between the sensor **L** and  $Mg^{2+}$ , IR spectra were collected, and the stretching vibration peak of (–C=O) in **L** at  $1605\text{ cm}^{-1}$  shifted to  $1619\text{ cm}^{-1}$  when **L** interacted with  $Mg^{2+}$  (Fig. S6†). These phenomena indicate that in **L**– $Mg^{2+}$ , the  $Mg^{2+}$  coordinated with the oxygen atoms on the acylhydrazone group.

An obtained mass spectrum confirmed that the sensor **L** ion peak was detected at  $m/z$  339.08, which corresponded to  $[L + H]^+$ , and the magnesium complex ion peak appeared at  $m/z$  439.09, which indicated that after deprotonation, probe **L** reacted with  $Mg^{2+}$  and one DMSO to form a stable complex  $[L - 2H^+ + Mg^{2+} + 1DMSO + 1H^+]^+$  (Fig. S7†). A job plot analysis showed a 1 : 1 stoichiometry for the **L**– $Mg^{2+}$  complex (Fig. 7). Based on the data in the job plot, <sup>1</sup>H NMR spectra and IR spectra, a stable complex between **L** and  $Mg^{2+}$  was proposed.

The sensing mechanism was estimated based on the above experiments. In solution, **L** exhibited weak fluorescence owing to ESIPT. The addition of  $Mg^{2+}$  broke the intramolecular

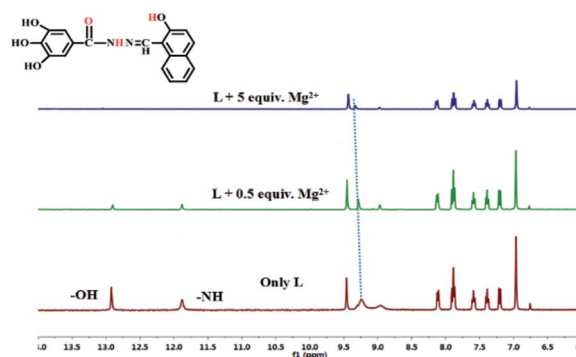


Fig. 6 <sup>1</sup>H NMR spectra of free **L** and in the presence of  $Mg^{2+}$ .

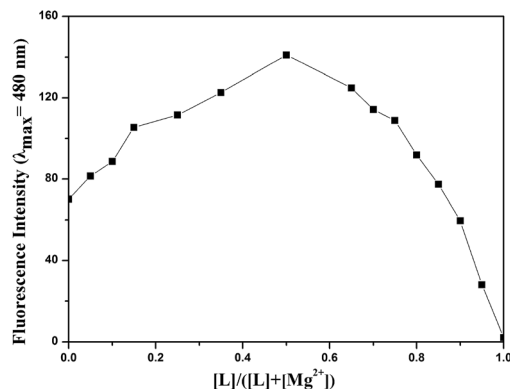


Fig. 7 Job plot of **L** with  $Mg^{2+}$ .



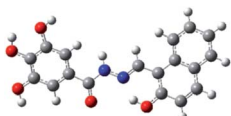
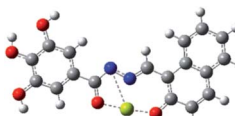
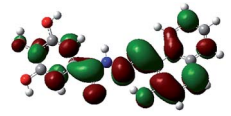
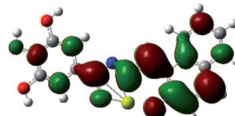
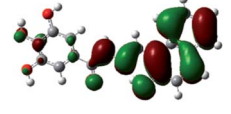
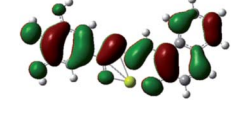
hydrogen bond and deprotonated the secondary amine. Hence, excited state intramolecular proton transfer was inhibited. The sensor **L** showed strong green fluorescence (Scheme 2).

In order to investigate the reversibility of the sensor **L**, the addition of  $Mg^{2+}$  to a solution of sensor **L** that had no fluorescence showed increasing fluorescence (That was "ON"). After adding of EDTA to the solution of **L**- $Mg^{2+}$  complex, there was no fluorescence (That was "OFF"). In fact, this "OFF-ON-OFF" switching process could be repeated several times with little fluorescent efficiency loss (Fig. 8).

To further confirm the proposed mechanism of sensor **L** with  $Mg^{2+}$ , we performed DFT calculations at the B3LYP/6-311g (2d, p) level of theory. The highest occupied molecular orbital (HOMO) and the lowest unoccupied molecular orbital (LUMO) of **L** and the **L** +  $Mg^{2+}$  complex were investigated and are shown in Table 2. The HOMO-LUMO energy band gap of **L** +  $Mg^{2+}$  complex was 0.12157 au, which was lower than that of **L** (0.13522 au).

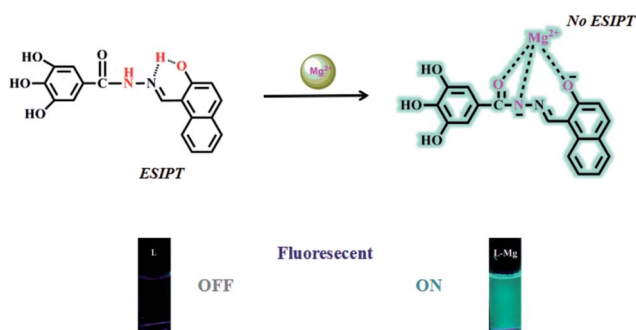
To investigate the practical application of chemosensor **L**, test strips were prepared by immersing filter papers into a DMSO/H<sub>2</sub>O (7 : 3, v/v, 0.01 M HEPES, pH = 8.5) solution of **L** (0.1 M) and then drying in air. The test strips containing **L** were utilized to sense  $Mg^{2+}$  and other metal ions. As shown in Fig. 9, when the test strips were added to solutions of  $Mg^{2+}$  and the other ions, a significant color change was observed only with

Table 2 Density functional theory results for **L** and **L** +  $Mg^{2+}$ <sup>a</sup>

	<b>L</b>	<b>L</b> + $Mg^{2+}$
Optimized structure		
Diagrams of LUMOs		
Diagrams of HOMOs		
Energy gaps	0.13522 au	0.12157 au

<sup>a</sup> Blue ball is nitrogen, grey ball is carbon, red ball is oxygen, yellow ball is magnesium, and white ball is hydrogen.

$Mg^{2+}$  solution under a 365 nm UV lamp. Moreover, potentially competitive ions exerted no influence on the detection of  $Mg^{2+}$  by the test strips. Therefore, the test strips based on **L** could quickly and conveniently detect  $Mg^{2+}$  in solutions. The practical



Scheme 2 A possible sensing mechanism of the sensor **L** with  $Mg^{2+}$ .

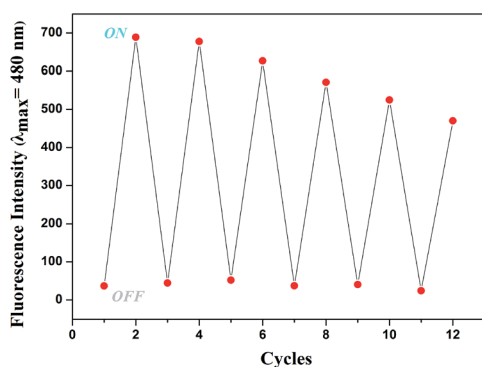


Fig. 8 Fluorescence experiment showing the reversibility and reusability of the **L** for sensing  $Mg^{2+}$ . Emission intensity changes at 480 nm for **L** upon addition of 10 equiv.  $Mg^{2+}$  before and after addition of 10 equiv. EDTA.

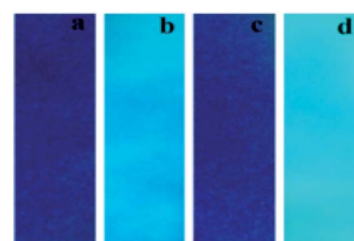


Fig. 9 Photographs of **L** on test strips (a) only **L**, (b) after immersion into solutions with  $Mg^{2+}$ , (c) after immersion into DMSO solutions with other cations, (d) after immersion into solutions with  $Mg^{2+}$  and other cations under irradiation at 365 nm.

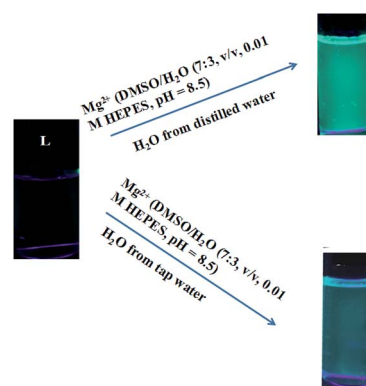


Fig. 10 Images of  $Mg^{2+}$  induced turn-on fluorescence in different sources of water.



application of sensor **L** for selective sensing of  $Mg^{2+}$  in two different sources of water, distilled and tap water, has also been demonstrated. The results showed that sensor **L** was a sensitive sensor and could be applied in environmental analysis (Fig. 10).

## Conclusions

In summary, we have developed a sensor that can detect  $Mg^{2+}$  ions in a weakly alkaline medium of DMSO/ $H_2O$  (7 : 3, v/v, 0.01 M HEPES, pH = 8.5) with high selectivity and special sensitivity. Moreover, the fluorescence detection limit was low  $9.2 \times 10^{-10}$  M for  $Mg^{2+}$ . In addition, **L** could be used as a novel NOR logic gate triggered by  $Mg^{2+}$  and EDTA. Test strips based on **L** were also fabricated, which could serve as a practical fluorescent sensor to detect  $Mg^{2+}$  in field measurements or in test kits. Thus, the probe could have potential applications in both environmental and biological systems for the monitoring of magnesium.

## Acknowledgements

This study was supported by the National Nature Science Foundation of China (No. 21467012).

## Notes and references

- G. Men, C. Chen, S. Zhang, C. Liang, Y. Wang, M. Deng, H. Shang, B. Yang and S. Jiang, *Dolton Trans.*, 2015, **44**, 2755.
- T. Dudev, K. Mazmanian and C. Lim, *Phys. Chem. Chem. Phys.*, 2016, **18**, 16986.
- H. S. Yin, B. C. Li, Y. L. Zhou, H. Y. Wang, M. H. Wang and S. Y. Ai, *Biosens. Bioelectron.*, 2017, **96**, 106.
- B. O'Rourke, P. H. Backx and E. Marban, *Science*, 1992, **257**, 245.
- J. Smith, *J. Am. Chem. Soc.*, 1927, **69**, 1492.
- L. Wang, W. Qin, X. Tang, W. Dou and W. Liu, *J. Phys. Chem. A*, 2011, **115**, 1609.
- H. O. Trowbridge and J. L. Seltzer, *J. Periodontal Res.*, 1967, **2**, 147.
- H. C. Politi and R. R. Preston, *Neuroreport*, 2003, **14**, 659.
- Y. Ma, H. Liu, S. Liu and R. Yang, *Analyst*, 2012, **137**, 2313.
- C. Berti, V. Zsolnay, T. R. Shannon, M. Fill and D. Gillespie, *J. Mol. Cell. Cardiol.*, 2017, **103**, 31.
- J. Orrego-Hernández, N. Nunez-Dallos and J. Portilla, *Talanta*, 2016, **152**, 432–437.
- L. Y. Shen, Y. H. Zhao, L. Mu, X. Zeng, R. Carl and G. Wei, *Sens. Actuators, B*, 2016, **226**, 279.
- M. Jamshidi, O. Rezaei, A. R. Belverdi, S. Malekian and A. R. Belverdi, *J. Mol. Struct.*, 2016, **1123**, 111.
- D. Ray and P. K. Bharadwaj, *Inorg. Chem.*, 2008, **47**, 2252.
- C. Y. Lu, Y. W. Liu, P. J. Huang, C. F. Wan and A. T. Wu, *Analyst*, 2013, **138**, 2527.
- S. Devaraj, Y. Tsui, C. Chiang and Y. Yen, *Spectrochim. Acta, Part A*, 2012, **96**, 594.
- R. Alam, T. Mistri, A. Katarkar, K. Chaudhuri, S. K. Mandal, A. R. K. Bukhsh, K. K. Das and M. Ali, *Analyst*, 2014, **139**, 4022.
- V. K. Gupta, A. K. Singh and L. K. Kumawat, *Sens. Actuators, B*, 2014, **204**, 507.
- D. Sarkar, A. K. Pramanik and T. K. Mondal, *J. Lumin.*, 2014, **146**, 480.
- B. B. Shi, P. Zhang, T. Wei, H. Yao, Q. Lin and Y. Zhang, *Chem. Commun.*, 2013, **49**, 7812.
- S. Wang, X. Fei, J. Guo, Q. Yang, Y. Li and Y. Song, *Talanta*, 2016, **148**, 229.
- Y. Sun, J. H. Hu, J. Qi and J. B. Li, *Spectrochim. Acta, Part A*, 2016, **167**, 101.
- D. S. Kopchuk, A. M. Prokhorov, P. A. Slepukhin and D. N. Kozhevnikov, *Tetrahedron Lett.*, 2012, **53**, 6265.
- Q. Lin, Y. P. Fu, P. Chen, T. B. Wei and Y. M. Zhang, *Dyes Pigm.*, 2013, **96**, 1.
- (a) J. Liu, Q. Lin, Y. M. Zhang and T. B. Wei, *Sens. Actuators, B*, 2014, **196**, 619; (b) G. Chen, Z. Guo, G. Zeng and L. Tang, *Analyst*, 2015, **140**, 5400.
- J. H. Hu, J. Qi, Y. Sun and P. X. Pei, *Phosphorus, Sulfur Silicon Relat. Elem.*, 2017, **192**, 565.
- P. Zhang, B. B. Shi, X. M. You, Y. M. Zhang, Q. Lin, H. Yao and T. B. Wei, *Tetrahedron*, 2014, **70**, 1889.
- H. M. Kim, P. R. Yang, M. S. Seo, J. S. Yi, J. H. Hong, S. J. Jeon, Y. G. Ko, K. J. Lee and B. R. Cho, *J. Org. Chem.*, 2007, **72**, 2088.
- Y. Liu, M. Han, H. Zhang, L. Yang and W. Jiang, *Org. Lett.*, 2008, **10**, 2973.
- E. J. Park, M. Brasuel, C. Behrend and M. A. Philbert, *Anal. Chem.*, 2003, **75**, 3784.
- P. S. Hariharan and S. P. Anthony, *RSC Adv.*, 2014, **4**, 41565.
- H. Sharma, N. Kaur, A. Singh, A. Kuwar and N. Singh, *J. Mater. Chem. C*, 2016, **4**, 5154.
- J. H. Hu, J. B. Li, J. Qi and Y. Sun, *Sens. Actuators, B*, 2015, **208**, 581.
- J. H. Hu, J. B. Li, J. Qi and Y. Sun, *New J. Chem.*, 2015, **36**, 4041.
- J. B. Li, J. H. Hu, J. J. Chen and J. Qi, *Spectrochim. Acta, Part A*, 2014, **133**, 773.
- J. H. Hu, N. P. Yan and J. J. Chen, *J. Chem. Res.*, 2012, **36**, 619.
- J. H. Hu, N. P. Yan, J. J. Chen and J. B. Li, *Chem. Res. Chin. Univ.*, 2013, **34**, 1368.
- J. Qi, J. H. Hu, Y. Sun and J. B. Li, *Curr. Anal. Chem.*, 2016, **12**, 119.
- G. Wang, J. Qin, L. Fan, C. Li and Z. Yang, *J. Photochem. Photobiol., A*, 2016, **314**, 29.
- J. Qin, Z. Yang and G. Wang, *Inorg. Chim. Acta*, 2015, **435**, 194.
- L. Jin, Z. Guo, Z. Sun, A. Li, Q. Jin and M. Wei, *Sens. Actuators, B*, 2012, **161**, 714.

